

# An in-Field Calibrating Method for the Bilateral Filter Applied to X-ray Flat Panel Grayscale Images with High Spectral Resolution

Fabiana Oliveira Paixão Fernandes<sup>1</sup>, Cássio Alves Carneiro<sup>2</sup>, Petr Iakovlevitch Ekel<sup>1</sup>,  
Zélia Myriam Assis Peixoto<sup>1</sup> and Flávia Magalhães Freitas Ferreira<sup>1</sup>

<sup>1</sup> Graduate Program in Electrical Engineering, Pontifical Catholic University of Minas Gerais,  
500 Dom José Gaspar Avenue, Belo Horizonte, Brazil

<sup>2</sup> University Center of Sete Lagoas, Sete Lagoas, Brazil

**Keywords:** Bilateral Filter, Image Denoising, X-ray Images, Flat Panel.

**Abstract:** Several spatial filters applied to images are available in technical and scientific literature. Besides the reduction of the noise level, some of them also aim at the preservation of edges and details. Those filters are commonly applied to the processing of X-ray medical image sequences, which are usually noised due to the low doses of radiation suitable for medical procedures but where the loss of any detail may impair a diagnosis. In this context, the bilateral filter is well suited. However, an adequate calibration of the bilateral filter is required for reaching the best cost benefit between reducing the noise level and preserving the image edges. Calibration procedures are still underexplored in the literature thereby, this paper proposes a new method that allows in-field calibration of the bilateral filter embedded into a piece of equipment for angiography, which uses a flat panel X-ray detector. The proposed method can be applied to images with any spectral resolution and surpasses the performance of the calibration method presented in the literature.

## 1 INTRODUCTION

The acquisition of X-ray images is carried out under strict conditions of exposure time of the patient to radiation and X-ray dosage. However, decreasing the dose implies increasing the image noise level suppressing important details and thus hindering the diagnosis. Therefore, denoising of medical X-ray images is of great importance as there is also the concern to preserve the characteristics of the image (Zhang et al., 2009).

In those cases, temporal filtering techniques are a good tool for preserving image details, beyond of its low complexity of implementation. However, in sequences of images where some movement is present, e.g. digital angiography for hemodynamic tests, the classic temporal filtering techniques cannot be applied, because they cause trails in the motion direction. Thus, spatial filters may be used instead.

These filters are accomplished with convolution masks applied to the pixels of the image. As a result they reduce the noise level but also cause edge smoothing usually. This shortcoming precludes their use for medical purposes since losses are not commonly allowed in accurate diagnosis. However,

some spatial filters are more likely to preserve edges. A suitable example is the bilateral filter, which combines a domain filter to a range filter. The first takes into account the spatial distance between neighboring pixels to calculate the mask weights, while the second is concerned about the difference between their gray intensities (Tomasi and Manduchi, 1998).

In (Gabiger-Rose et al., 2011) a procedure to calculate the parameters of the bilateral filter for grayscale images with spectral resolution of 8 bits was proposed. However, there are few works in the literature that carry out studies on the application of the bilateral filter to medical images with high spectral resolution, e.g., 14 bits.

In this paper, major concerns of the authors are to guarantee an industrial in-field calibration method for bilateral filter embedded into medical apparatus of angiography that are built with an X-ray flat panel detector. Nowadays the denoising process applied in this kind of equipment to process sequences of moving images is the same as 50 years ago, i.e., consisting of same classical spatial filters, such as the averaging filter. Firstly our study proposes a slight modification into the equations for the filter's

parameters presented in Gabiger-Rose et al., (2011) in order to extend the adjusting method of the parameters to images with any bit resolution. However, the largest contribution is the change in that calibration methodology itself which results in major gains in quality metrics when comparing to the method of Gabiger-Rose et al., (2011).

This paper is organized as follows. After a brief introduction of the bilateral filter in Section 2, a short overview of the calibration method described in Gabiger-Rose et al., (2011) is given in Section 3. The proposed contributions that allow the in-field calibrating method can be seen in Section 4. Section 5 shows experimental results already obtained and in Section 6 one can find the conclusion of this work.

## 2 BILATERAL FILTER

The bilateral filter was firstly proposed by Tomasi and Manduchi (1998) consisting of a discrete filter applied in the spatial domain by using a convolution mask, according to the Equation (1),

$$y(k) = \frac{\sum_{n=-N}^N W(k,n)x(k-n)}{\sum_{n=-N}^N W(k,n)} \quad (1)$$

where  $W(k,n)$  weighs the contribution of each neighboring pixel  $x(k-n)$  inside the mask regarding the calculation of the value of the processed pixel  $x(k)$ ,  $k$  is the location of the central pixel of the mask and  $n$  is the distance between the central pixel and its neighbor. The two-dimensional filtering can be performed in two one-dimensional steps.

In the bilateral filter, the contribution  $W(k,n)$  of each neighboring pixel corresponds to the product of the weight  $W_d(n)$  of a domain filter that depends on the spatial distance between the two pixels and on the weight  $W_r(k,n)$  of a range filter that depends on the difference between the intensities of both (Giraldo et al., 2009). The weights  $W_d(n)$  and  $W_r(k,n)$  are determined by Equations (2) e (3), in which  $\sigma_d$  and  $\sigma_r$  are adjusting parameters of the decay curve of the filters weights in function of the spatial distance  $n$  and of the difference of intensities  $x(k-n)$  and  $x(k)$ , respectively. The idea is that even neighboring pixels very close, but very different in intensity, provide a small contribution in the result of the spatial filtering. Thus, the image edges are better preserved and the noise level is reduced mainly in the regions in which intensity levels are more uniform.

$$W_d(n) = \exp\left(-\frac{n^2}{2\sigma_d^2}\right) \quad (2)$$

$$W_r(k,n) = \exp\left(-\frac{(x(k)-x(k-n))^2}{2\sigma_r^2}\right) \quad (3)$$

The calibration of the bilateral filter consists of determining the parameters  $\sigma_d$  and  $\sigma_r$ . It is necessary to reach the best-cost benefit between reducing the noise level and preserving the image edges, objectives that are conflicting in nature.

## 3 ADJUSTMENT

### 3.1 Domain Filter

In Gabiger-Rose et al., (2011) it was presented a method for the adjustment of the parameter  $\sigma_d$ , which depends only on the size of the convolution mask. In order to approximate an ideal low-pass filtering, the authors claim that the weighting coefficients that would be outside the mask have to be smaller than or equal to  $10^{-3}$ . This condition is expressed in Equation (4), in which the size of the one-dimensional mask is  $2N+1$ .

$$\max\left(W_d(n)\Big|_{n \in N}\right) \leq 10^{-3} \quad (4)$$

For a convolution mask of dimension  $7 \times 1$ , which proved to be in our experiments the most appropriate for filtering purposes, the calculated value for the parameter  $\sigma_d$  obeying Equation 4, with  $N=3$  and  $n=4$ , was 1.08.

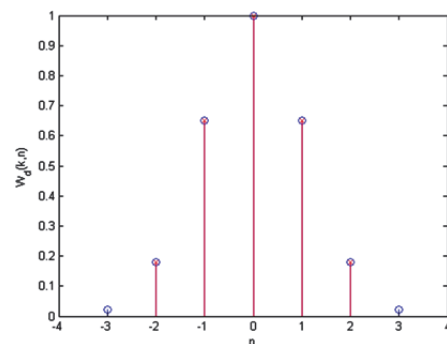


Figure 1: Weights of masks  $5 \times 1$  and  $7 \times 1$  using  $\sigma_d=1.08$ .

However, if  $\sigma_d$  is equal to 1.08 in the  $7 \times 1$  mask, the value of the last coefficient inside the mask ( $n=3$ ) is very close to zero. Our first criticism of the method refers to the mask  $7 \times 1$  behaving very similarly to the mask  $5 \times 1$  as it can be observed in

Figure 1, which depicts the weights  $W_d(n)$ , for  $n$  varying from  $-N$  to  $+N$ , for masks  $7 \times 1$  (blue circles) and  $5 \times 1$  (red bars).

### 3.2 Range Filter

The parameter  $\sigma_r$  must be adjusted based on the level of noise present in the image in order to reach the best-cost benefit between reducing the noise level and preserving the image edges.

Thus, in Gabiger-Rose et al., (2011) it was proposed the determination of the parameter  $\sigma_r$  as the product of the noise standard deviation and a factor  $R$  (Equation 5) which must be determined in order to maximize either of the quantitative performance metrics. The suggested metrics are the PSNR (Peak Signal to Noise Ratio) and the MSSIM (Mean Measure Structural Similarity) (Wang et al., 2004), as a means of gaining perceptual proximity with the Human Visual System (HVS). While PSNR is measured in dB, MSSIM varies between 0 and 1 and evaluates quantitatively how close the output image is of a reference image, in terms of intensity, structure and contrast. Best results reflect on values of MSSIM near 1.

$$\sigma_r = R * \sigma_{noise} \quad (5)$$

To check the dependence of  $R$  in relation to the statistical characteristics of noise, Gabiger-Rose et al., (2011) used a test database composed by 50 images of 8-bit whose pixels were not normalized, where it was included an additive Gaussian noise of zero mean and variable standard deviation  $\sigma_{noise}$  (variation in the range of 1 to 64, in steps of 4). Images were filtered using a bilateral filter with fixed  $\sigma_d$  (calculated using Equation 4) and with  $\sigma_r$  calculated according to Equation (5), trying values of  $R$  in the range of 0.5 to 16, in steps of 0.5. The metrics PSNR and MSSIM are calculated separately for each image, and finally, the average of these metrics, considering all the images for each pair  $(\sigma_{noise}, R)$  is determined. These mean values then become the characteristic values of the metrics for each specific pair  $(\sigma_{noise}, R)$ . The idea is to choose the parameter  $R$  that maximizes both characteristic metrics, for each value of the parameter  $\sigma_{noise}$ .

In order to highlight the differences among the characteristic metrics obtained by using different values of  $R$ , the characteristic metrics which refer to a specific  $\sigma_{noise}$  are normalized in relation to the maximum value of that same set, in accordance with Equation 6. Thus, the highest value of the characteristic metrics for a specific  $\sigma_{noise}$  is mapped to the value 1 and its null value is mapped to the

value 0. If we generate a grayscale image aiming at easier viewing and interpretation of these values, the dark line at this image corresponds to the best performance for different  $\sigma_{noise}$ . Figure 2 shows the visualization of data relating to the normalized characteristic PSNR.

$$metrics_{norm} = \left( 1 - \frac{metrics_{average}}{metrics_{max}} \right)^{0.2} \quad (6)$$

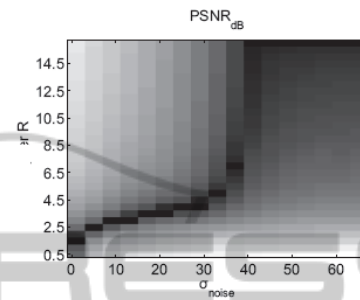


Figure 2: Normalized characteristic PSNR as a function of  $R$  and  $\sigma_{noise}$  (Gabiger-Rose et al., 2011).

## 4 SENSITIVITY ANALYSIS OF THE BILATERAL FILTER AND THE IN-FIELD CALIBRATION

Unlike Gabiger-Rose et al., (2011), that found the most presumably suitable parameter  $\sigma_d$  according to Equation 4 and kept this value invariant while seeking the optimal  $R$  for different  $\sigma_{noise}$ , our method consists in applying a sensitivity analysis of the filter regarding the parameters  $\sigma_d$  and  $R$ , in order to improve the adjustment of these parameters aiming at optimizing either of the metrics, at a specific level of  $\sigma_{noise}$ .

Furthermore, the calibration method presented in Gabiger-Rose et al. (2011) was applied only to 8 bits grayscale images. However, medical images are generally encoded with 14 bits. Thereby, in order to make the calibration procedure independent of spectral resolution, we first normalize the image pixels between 0 and 1.

In the calibration procedure, an industrial phantom acquired in real conditions of medical procedures must be used due to the need for having sequential multiple still images in order to find a reference image, presumably noise-free, for the calculation of the metrics. This procedure is not possible with real medical images since it would submit the patient to long exposures to X-rays. The calibration phantom must have density

characteristics that simulate different tissues of the human body as well as frequency components that simulate structures present in the medical procedures such as blood vessels, bone structures, calcifications and catheters. The phantom image is processed by bilateral filter and the filtered image is compared to the reference image in order to compute the metrics. The reference image is obtained from a temporal average of 8 frames of the calibration phantom, acquired at different times. The value of  $\sigma_{noise}$ , necessary to compute  $\sigma_r$  in accordance with Equation 5 is estimated from the histogram of the difference between one of the noisy image frames and the reference image after normalizing their pixels.

In our experiments, the calibration phantom image shown in Figure 3 was acquired with the equipment AngiX III FD, manufactured by Brazilian company Xpro. The estimated value for  $\sigma_{noise}$  was 0.026. The sensitivity analysis with respect to the filter parameters was performed by varying both  $\sigma_d$  and  $R$ . The first varied from 0.5 to 5, in steps of 0.5 and the second varied from 0.5 to 10, in steps of 0.5. The metrics PSNR and MSSIM were calculated for the calibrating phantom image for each  $(\sigma_d, R)$  pair.

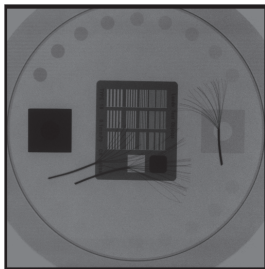


Figure 3: Calibrating phantom image.

Figures 4 and 5 provide visualization of PSNR and MSSIM gains for helping with the analysis of filter sensitivity to the parameters adjustment in which the hot colors correspond to positive gains while the cold colors correspond to negative gains, respectively. The metrics gain refers to the difference between the metrics for the filtered image and the metrics for the noisy image, before the application of the filter. The graphs in Figures 6 and 7, in turn, correspond to the metrics (PSNR and MSSIM, respectively) normalized in accordance with Equation (6), where  $metrics_{max}$  corresponds to the maximum value of each metrics for a fixed value of  $\sigma_d$ . These figures do not intend to compare the performance of the filter to each  $(\sigma_d, R)$  pair. Instead, they just give an insight into the determination of the optimum  $R$  for a specific value

of  $\sigma_d$ , since they assign, with a zero value in the  $z$ -axis, the value of  $R$  that optimizes the filter performance at each  $\sigma_d$ .

From Figures 4 and 5, it can be noticed that the best performance of the bilateral filter is achieved for larger values of  $\sigma_d$ , which contradicts the choice of the parameter  $\sigma_d$  proposed in Gabiger-Rose et al. (2011).

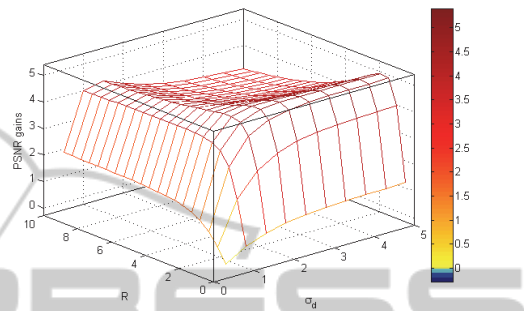


Figure 4: PSNR gains (dB) as a function of  $\sigma_d$  and  $R$  using the calibrating phantom.

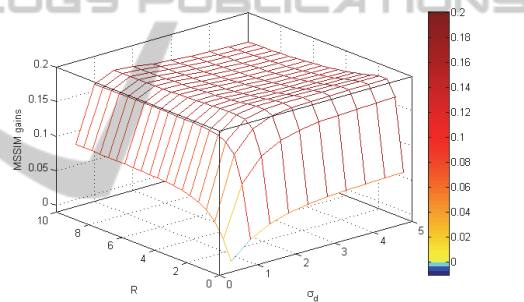


Figure 5: MSSIM gains as a function of  $\sigma_d$  and  $R$  using the calibrating phantom.

From Figures 6 and 7, it can be verified that the lower the value of  $\sigma_d$ , the larger the expected value of  $R$  aiming at optimizing performance. However, for values of  $\sigma_d$  greater 2.5, the optimum  $R$  does not change and it is equal to 2 for the calibration phantom.

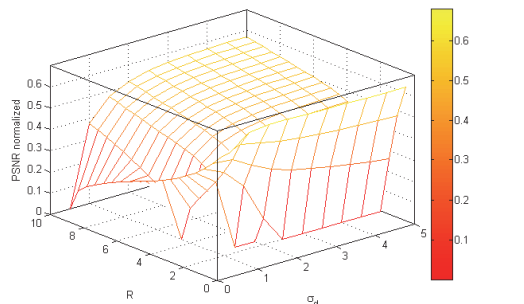


Figure 6: Normalized values for PSNR (dB) as a function of  $\sigma_d$  and  $R$  using the calibrating phantom.



It is worth noticing that the classic average filter is equivalent to the bilateral filter with the highest values of  $\sigma_d$  and  $R$ . In other words, it corresponds to the worst performance of the bilateral filter.

It is concluded from the proposed calibration method and using the shown calibration phantom, we choose to adjust the two parameters of the bilateral filter with values  $\sigma_d = 3$  and  $R=2$ , using a  $7 \times 7$  convolution mask.

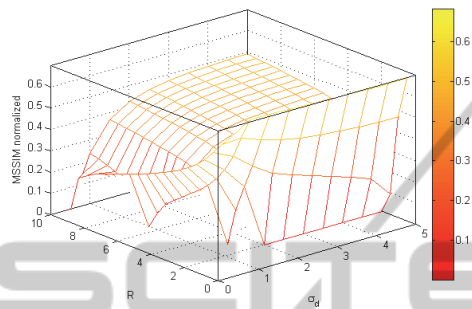


Figure 7: Normalized values for MSSIM as a function of  $\sigma_d$  and  $R$  using the calibrating phantom.

## 5 RESULTS

The in-field calibrated bilateral filter (implemented in Matlab) was then used to reduce the noise level at the image of a test phantom, shown in Figure 8, also acquired by AngiX III FD in equivalent conditions of real medical procedures. The achieved gains of PSNR and MSSIM are shown in Table 1 at three different conditions: first,  $\sigma_d = 1.08$  and  $R=5$  which are the values found through the method presented in Gabiger-Rose et al., (2011); second,  $\sigma_d = 3$  and  $R=2$  which are the optimum values found by our calibrating method; and third,  $\sigma_d = 3$  and  $R=10$  which corresponds to the classic average filter for which the PSNR presented a decrease of 0.231dB.

Table 1: PSNR and MSSIM gains using the test phantom.

$\sigma_d$	R	PSNR gains	MSSIM gains
Gabiger-Rose et al. (2011)			
1.08	5	2.7093	0.0948
Our in-field calibratin method			
3	2	3.0753	0.1085
Classic average filter			
3	10	-0.231	-0.0327

Making a subjective analysis on images of Figure 8, it is noticed that with  $\sigma_d = 3$  and  $R=10$  the image is plainly blurry, that is, visible losses occur at the edges. With the method presented in Gabiger-Rose et al., (2011),  $\sigma_d = 1.08$  and  $R=5$ , the noise

level is not reduced as expected.

The bilateral filter was also applied on a real medical image with 14 bits, shown in Figure 9. Although the metrics PSNR and MSSIM cannot be calculated due to the lack of the reference image, we compared the performance of our in-field calibration procedure to the performance of the method presented in Gabiger-Rose et al., (2011) by analyzing the visual quality of the filtered images.

Visual inspection of the image obtained from the classic average filter is also performed. It can be noted that the perceptual analysis carried out for the real medical image leads to the same achievements gotten for the test phantom.

## 6 CONCLUSIONS

The bilateral filter is used in several recent papers and it is notable for owning the feature of preserving edges. However, the literature lacks a clear and efficient procedure to calibrate the parameters of this filter. The majority of papers that process grayscale images encoded with 8 bits only mentions the values of the used parameters of the filters and do not show the way they were determined. Fortunately, from the calibration procedure presented in Gabiger-Rose et al., (2011) for 8 bits images, we were able to generalize the original proposal to the case of images with any spectral resolution. Besides that, we present a more accurate industrial in-field procedure to find the values of the parameters of the filter that optimize either PSNR or MSSIM using a phantom image acquired by the X-ray flat panel equipment itself. The denoising process of X-ray images using the bilateral filter properly calibrated gave us a superior result in terms of noise level reduction and edge preservation, when comparing to works presented in recent literature. This was verified not only from metrics calculated from phantom images but also from visual inspection of filtered real medical images. It is important to stress that our proposal is that this industrial in-field calibration procedure can be applied in practical operation conditions of medical pieces of equipment of angiography that use X -ray flat panel detector. The method intends to provide X-ray images with higher quality independent of flat panel manufacturer, as well as of total harmonic distortion of the network power distribution and of other parameters that influence the quality of the acquired images, like local temperature and humidity.

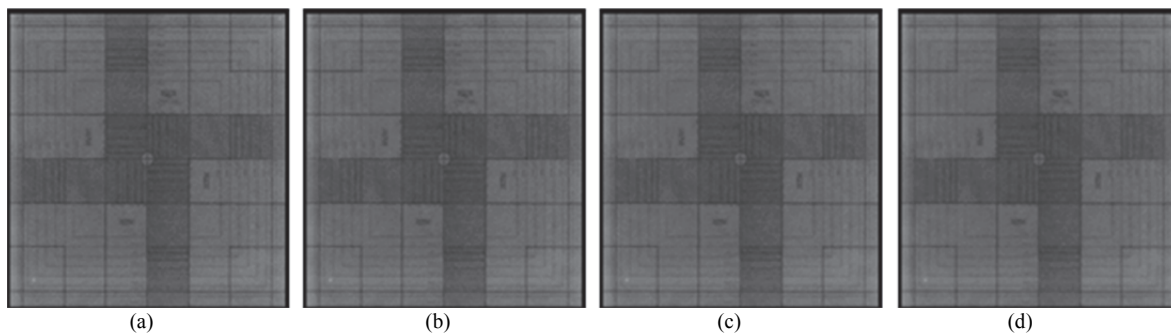


Figure 8: Test phantom (a) noisy image (b) denoised image:  $\sigma_d = 1$  and  $R=5$  (c) denoised image:  $\sigma_d = 3$  and  $R=2$  (d) denoised image:  $\sigma_d = 3$  and  $R=10$ .

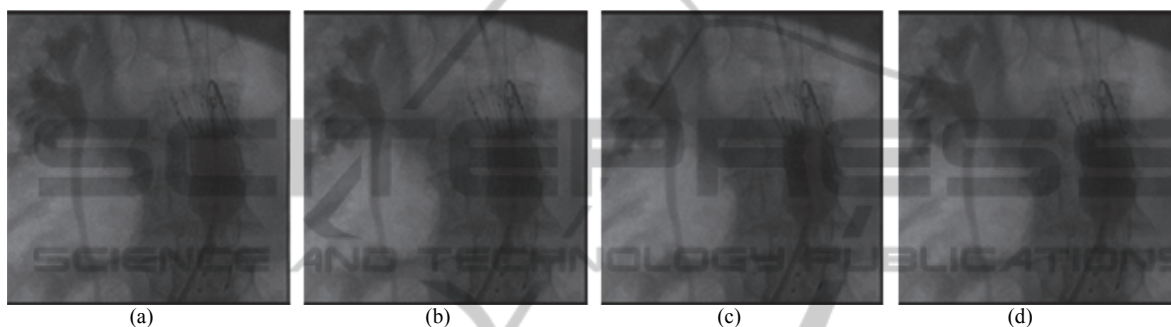


Figure 9: Medical Image (a) noisy image (b) denoised image:  $\sigma_d=1$  and  $R=5$  (c) denoised image:  $\sigma_d=3$  and  $R=2$  (d) denoised image:  $\sigma_d=3$  and  $R=10$ .

## REFERENCES

- Gabiger-Rose, A., Kube, M., Schmitt, P., Weigel, R., & Rose, R., (2011). Image Denoising Using Bilateral Filter With Noise-Adaptive Parameter Tuning. *37th Annual Conference on IEEE Industrial Electronics Society*.
- Giraldo, J., Kelm, Z., Guimaraes, L., Yu, L., Fletcher, J., Erickson, B. and McCollough, C., (2009). Comparative Study of Two Image Space Noise Reduction Methods for Computed Tomography: Bilateral Filter and Nonlocal Means. *31st Annual International Conference of the IEEE EMBS*. Minneapolis, Minnesota, USA.
- Tomasi, C., and Manduchi, R., (1998). Bilateral Filtering for Gray and Color Images. *IEEE International Conference on Computer Vision*. Bombay, India.
- Wang, Z., Bovik, A., Sheikh, H. and Simoncelli, E., (2004). Image Quality Assessment: From Error Visibility to Structural Similarity. *IEEE Transactions on Image Processing*, 13, 600-612.
- Zhang, L., Chen, J., Zhu, Y. and Luo, Z., (2009). Comparisons of Several New De-Noising Methods for Medical Images. *3rd International Conference on Bioinformatics and Biomedical Engineering*.